International Journal of Nanomedicine

Dovepress
open access to scientific and medical research

Open Access Full Text Article

ORIGINAL RESEARCH

Antibiotic-Polyphosphate Nanocomplexes: A Promising System for Effective Biofilm Eradication

Dennis To[1], Mariana Blanco Massani[1], Débora C Coraça-Huber[2], Anna Seybold[3], Fabrizio Ricci[1,4], Katrin Zöller[1], Andreas Bernkop-Schnürch[1]

[1]Center for Chemistry and Biomedicine, Department of Pharmaceutical Technology, Institute of Pharmacy, University of Innsbruck, Innsbruck, Austria; [2]Research Laboratory for Implant Associated Infections (BIOFILM LAB), Experimental Orthopaedics, University Hospital for Orthopaedics and Traumatology, Medical University Innsbruck, Innsbruck, Austria; [3]Department of Zoology, University of Innsbruck, Innsbruck, Austria; [4]Thiomatrix Forschungs- und Beratungs GmbH, Innsbruck, Austria

Correspondence: Andreas Bernkop-Schnürch, Email Andreas.Bernkop@uibk.ac.at

Purpose: The eradication of bacterial biofilms poses an enormous challenge owing to the inherently low antibiotic susceptibility of the resident microbiota. The complexation of antibiotics with polyphosphate can substantially improve antimicrobial performance.

Methods: Nanoparticular complexes of the model drug colistin and polyphosphate (CP-NPs) were developed and characterized in terms of their particle size and morphology, polydispersity index (PDI), zeta potential, and cytotoxicity. Enzyme-triggered monophosphate and colistin release from the CP-NPs was evaluated in the presence of alkaline phosphatase (AP). Subsequently, antimicrobial efficacy was assessed by inhibition experiments on planktonic cultures, as well as time-kill assays on biofilms formed by the model organism *Micrococcus luteus*.

Results: The CP-NPs exhibited a spherical morphology with particle sizes <200 nm, PDI <0.25, and negative zeta potential. They showed reduced cytotoxicity toward two human cell lines and significantly decreased hemotoxicity compared with native colistin. Release experiments with AP verified the enzymatic cleavage of polyphosphate and subsequent release of monophosphate and colistin from CP-NPs. Although CP-NPs were ineffective against planktonic *M. luteus* cultures, they showed major activity against bacterial biofilms, outperforming native colistin treatment. Strongly elevated AP levels in the biofilm state were identified as a potential key factor for the observed findings.

Conclusion: Accordingly, polyphosphate-based nanocomplexes represent a promising tool to tackle bacterial biofilm.

Keywords: polyphosphate, colistin, antimicrobial, nanoparticle, nanocomplex

Introduction

Biofilms are complex multicellular microbial living communities that represent one of the most widespread and predominant living patterns in existence.[1] A vast number of microorganisms can attach to a surface and grow as biofilm, forming three-dimensional structures at various interfaces. The residing microbiota grows at a high cell density and excretes a matrix of extracellular polymeric substances (EPS) surrounding and protecting microorganisms living in the biofilm. Biofilm colonies are typically characterized by tremendously reduced antibiotic susceptibility.[2] Although an antibiotic agent can be highly effective against planktonic microbes, it can be rendered useless once it encounters a biofilm infection. Moreover, biofilms can simultaneously host multiple microbial species. According to the National Institute of Health 65% of all microbial illnesses and 80% of chronic infections are associated with biofilm formation.[3] Biofilm formation occurs similarly on medical devices, such as catheters, heart valves or prostheses as well as on various body surfaces, eg mucosal membranes of the digestive and respiratory tract.[4] Nonetheless, there is no current consensus on the mechanism of biofilm resistance as biofilms still remain poorly understood. Multiple factors appear to be involved, including alterations in metabolism and growth rate, the activation of species-specific resistance genes and an insufficient penetration of the antibiotic inside the biofilm due to protection by the biofilm-matrix.[5,6] Owing to the multifactorial nature of biofilm tolerance to antibiotics, the treatment of biofilm-associated infections is very challenging, and the use of

Received: 12 June 2024
Accepted: 12 June 2024
Published: 18 September 2024

Graphical Abstract

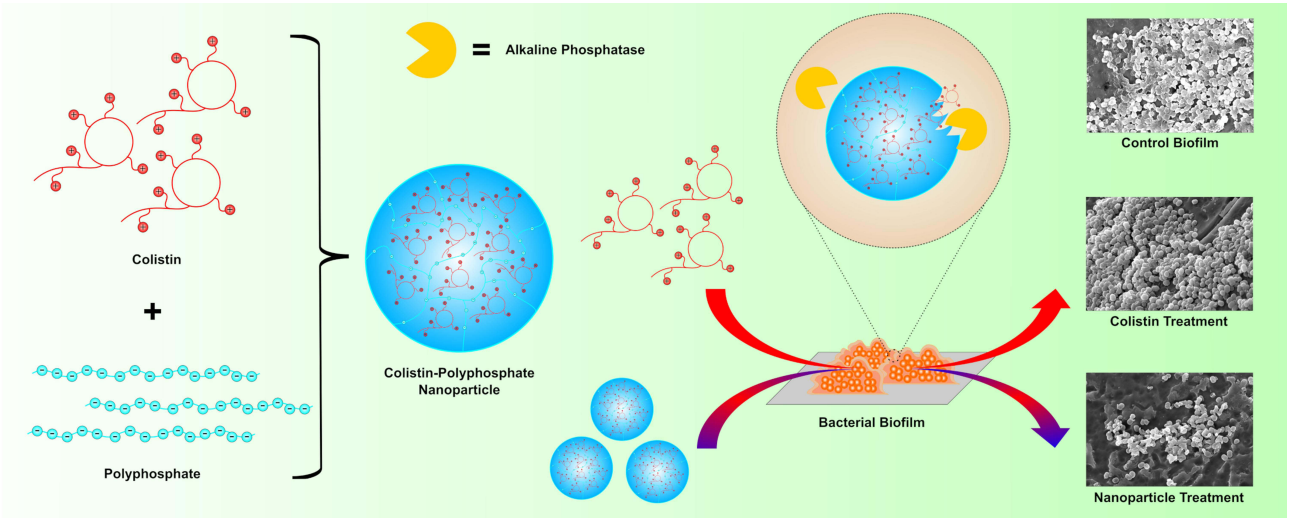

combination therapies is often required. Among the antibiotic agents used, particularly those exhibiting cationic charges, such as the peptide colistin, are prone to losing antimicrobial efficacy in the presence of biofilms. Electrostatic interactions with negatively charged components of the biofilm matrix, such as extracellular DNA (eDNA) or polysaccharides, can hinder or at least delay the penetration of the antibiotic, and might be a key reason for minor efficiency.[4,7–9]

Identifying and consequently targeting unique biofilm characteristics was proposed as a possible strategy to improve conventional antibiotic therapy and ameliorate eradication of biofilms.[5] Our research group has recently focused on the development of antibiotic-polyphosphate nanoparticular complexes as an efficient way to improve the systemic administration of antibiotic drugs.

Our research group has recently focused on the development of antibiotic-polyphosphate nanoparticular complexes as an efficient way to improve the systemic administration of antibiotic drugs. The incorporated polyphosphate structures are cleaved by the naturally occurring enzyme alkaline phosphatase (AP), leading to particle degradation and release of monophosphate and the associated drug. Polyphosphate-based nanoparticles were shown to have several advantages over unmodified drugs such as protection from enzymatic degradation, enhanced mucus permeation or enzyme-triggered drug release.[10–12] Furthermore, these nanocarriers proved to be effective for the delivery of antifungal drugs[13] and can exhibit increased cellular uptake.[14]

While the high potential of these systems for drug delivery is undoubted, surprisingly little is known about their inherent antimicrobial efficacy. In particular, their interactions with bacteria and bacterial biofilms have never been investigated to date.[15] Hence, also the impact of the bacterial biofilm matrix on the antimicrobial efficacy of these nanoparticles remains unknown. Given the urgent need for new antibiotic treatment options to combat persistent bacterial infections, it is of utmost importance to obtain further insight into the antimicrobial potential of polyphosphate-based nanocarriers. Therefore, this study aimed to develop antibiotic-polyphosphate nanoparticles and study their antimicrobial potential, with a special emphasis on bacterial biofilms. As a model drug, we chose the lipopeptide colistin, which is mainly active against gram-negative bacteria but also has certain activity against gram-positive bacteria.[16–18] Due to the polycationic nature of colistin, it should be able to interact electrostatically with the anionic substructures of polyphosphate, ideally forming complexes in the nanometer range.

As a model germ, we chose the prominent bacterium *Micrococcus luteus* which is a natural commensal bacterium of the human body. Although typically considered mildly virulent, *M. luteus* is a strong biofilm producer on various surfaces

and can cause severe opportunistic infections in some patients.[19–22] Furthermore, it is known that *M. luteus* possesses AP activity.[23]

The viability of the biofilms during incubation with the nanoparticles was assayed by determining colony-forming units (CFU), biomass, metabolic activity as well as AP activity. Additionally, scanning electron microscopy (SEM) was performed to investigate potential differences in biofilm morphology.

Materials and Methods

Materials

Colistin sulfate was purchased from Sanova Pharma, Austria. Sodium polyphosphate (PP, Graham's salt, n=25), alkaline phosphatase (AP) from bovine intestinal mucosa (≥10 U/mg solid), malachite green oxalate (MLG), 2,4,6-trinitrobenzenesulfonic acid solution (TNBS, 5% methanolic solution), D-glucose anhydrous, ammonium molybdate tetrahydrate, resazurin sodium salt, fetal bovine serum (FBS), potassium phosphate monobasic (KH_2PO_4), crystal violet, 3-(4,5-dimethylthiazol-2-yl)-2,5-diphenyltetrazolium bromide (MTT), minimum essential medium (MEM), magnesium chloride ($MgCl_2$), Triton X-100, sodium periodate ($NaIO_4$), 4-nitrophenyl phosphate and p-nitrophenol were purchased from Sigma-Aldrich, Austria. Spectra Por® Float-A-Lyzer® dialysis tubes cut-off: 300 kDa, 4-(2-hydroxyethyl)-1-piperazineethanesulfonic acid (HEPES), tryptic soy agar (TSA) and tryptic soy broth (TSB) were purchased from Carl Roth, Germany. Penicillin/streptomycin solution and phosphate-buffered saline (PBS) were purchased from Pan-Biotech, Germany. Erythrocyte concentrate was kindly donated by Tirol Kliniken, Austria. ColiRollers™ plating beads, Ultracel® - 100 K Membrane (cut-off: 100 kDa) and 2-amino-2-methyl-1-propanol were purchased from Merck, Germany. TripLE™ Express Enzyme and DNase I (100 U/mL) were obtained from Thermo Fisher Scientific, Austria. Leit-C was purchased from Plano GmbH, Wetzlar, Germany. All other reagents were of analytical grade and obtained from commercial sources.

Formation and Characterization of the Nanoparticles

Nanoparticle Formation by Ionic Gelation

Colistin-polyphosphate nanoparticles (CP-NPs) were formed by complexing cationic colistin with anionic polyphosphate via ionic gelation as previously described.[13,24] Therefore, colistin was dissolved in a concentration of 1 mg/mL, whereas PP was dissolved in a concentration of either 0.4 mg/mL, 0.6 mg/mL or 0.8 mg/mL. Different aqueous media were evaluated for complexation including demineralized water, 0.01 M HCl, 20 mM HEPES buffer pH 6.8 and 20 mM HEPES buffer pH 7.4. An aliquot of 500 µL of the colistin solution was added dropwise to 500 µL of PP solution at room temperature while stirring at 800 rpm with a Thermomixer (Thermomixer, Eppendorf, Germany). The mixture was incubated for 30 min on the Thermomixer. Subsequently, size, polydispersity index (PDI) and zeta potential of the prepared colistin-polyphosphate complexes were measured using a Zeta Sizer (Zetasizer Nano ZSP, Malvern Panalytical, UK).

Determination of Complexation Efficiency

A suitable formulation was selected based on the screening results and the incorporation of colistin into the nanocomplex was verified by centrifugation of the nanoparticle solution at 13,400 rpm for 10 min using a centrifugal membrane insert (Ultracel® - 100 K Membrane: cut-off 100 kDa, Merck). Thereafter, an aliquot of 50 µL of the centrifugate was subsequently mixed with 50 µL of a 0.01% TNBS solution in 0.1 M $NaHCO_3$ and incubated for 45 min at 37 °C to visualize the presence of primary amines. Corresponding absorbance was read at 450 nm using a plate reader (Tecan Spark™, Tecan Trading AG, Switzerland).[25] A calibration curve with free colistin was established to calculate the amount of free colistin in the centrifugate. The complexation efficiency was calculated according to Equation (1):

$$Complexation\ Efficiency\ (\%) = \frac{c(colistin\ initial) - c(colistin\ centrifugate)}{c(colistin\ initial)} x100\% \quad (1)$$

Energy-Filtered Transmission Electron Microscopy (EFTEM)

EFTEM was performed to visualize the morphology of CP-NPs as previously described.[11] Briefly, a freshly prepared solution of CP-NPs was diluted 1:10 with sterile water and 5 µL of the sample was mounted on a 200 mesh, Formvar/carbon-coated copper grid (Balzers Union, Liechtenstein). The sample was dried and subsequently analyzed using a Zeiss Libra 120 transmission electron microscope (Carl Zeiss AG, Oberkochen, Germany) equipped with a 2 × 2k high-speed camera and ImageSP software (Troendle, Germany).

Evaluation of Enzyme-Triggered Change in Size and Zeta Potential

Changes in the size and zeta potential of the CP-NPs in the presence and absence of AP were investigated. An aliquot of 1 mL of nanoparticle solution ($c_{Colistin}$ = 500 µg/mL) prepared in 20 mM HEPES buffer pH 7.4 was mixed with 20 µL of enzyme solution (10 U/mL) or (1 U/mL) resulting in final AP concentrations of 0.2 U/mL and 0.02 U/mL, respectively. The control was mixed with 20 µL of 20 mM HEPES buffer pH 7.4. The samples were incubated for seven days at 500 rpm and 37 °C on a Thermomixer. At predetermined time points, size, PDI and zeta potential were measured using the Zeta Sizer.

Evaluation of Enzyme-Triggered Release Kinetics

Release of Monophosphates

AP-triggered cleavage of monophosphate from CP-NPs was evaluated using a previously published protocol involving the malachite green assay with minor adjustments.[13] First, the nanoparticle solution prepared according to Section 2.2 was diluted 1:50 in 20 mM HEPES buffer pH 7.4 to fit into the linear range of the assay. Subsequently, phosphate release was induced by addition of AP (final AP concentrations 0.2 U/mL and 0.02 U/mL). As negative control, 20 mM HEPES buffer pH 7.4 was added instead. The samples were incubated for seven days at 500 rpm and 37 °C on a Thermomixer. At predetermined time points, 100 µL of each sample were withdrawn, mixed with 5 µL of 3.6 M sulfuric acid and frozen at −20 °C to stop enzyme activity. Malachite green reagent was freshly prepared by mixing first 8.5 mL of a 0.15% (m/V) 3.6 M H_2SO_4 with 340 µL of an 11% (m/V) Triton X-100 solution. Subsequently, 5.1 mL of an 8% (m/V) ammonium molybdate solution was added dropwise under continuous stirring with a magnetic stirrer. Finally, the frozen samples were thawn and aliquots of 50 µL were added to the wells of a 96-well plate. An aliquot of 50 µL of MLG reagent was added to each well, and the resulting absorbance was measured at 630 nm using the Tecan. A calibration curve with increasing amounts of KH_2PO_4 was established to calculate the amount of free monophosphate at each time point.

Release of Colistin

The release of colistin from CP-NPs in the presence and absence of AP was evaluated via dialysis setup. An aliquot of 1.5 mL of CP-NPs solution ($c_{Colistin}$ = 500 µg/mL) was added into a dialysis tube (cut-off: 300 kDa). The positive control consisted of 1.5 mL of colistin solution (500 µg/mL) included inside a separate dialysis tube. A 50 mL Falcon tube was used as a release reservoir and 15 mL of 20 mM HEPES buffer pH 7.4 was added as the release medium. Incubation was performed in a shaking incubator for seven days at 100 rpm and 37 °C. After predetermined time points, 100 µL was withdrawn from the release medium and immediately frozen at −20 °C. Subsequently, 100 µL HEPES buffer pH 7.4 was added to the release medium.

Enzyme-triggered colistin release from CP-NPs was evaluated by adding AP to the solution in the inner as well as in the outer chamber of the dialysis setup in final concentrations of 0.2 U/mL and 0.02 U/mL, respectively. After withdrawing and freezing aliquots of 100 µL, the release medium was replaced with 100 µL of HEPES buffer pH 7.4 containing the respective concentrations of AP.

After collection of all aliquots, the samples were thawn and 50 µL of each sample was pipetted into a 96-well plate. The amount of free, released colistin was determined using the TNBS assay as described above. Blank values of pure buffer and buffer containing AP in the concentrations 0.2 U/mL and 0.02 U/mL were recorded and subtracted from the corresponding absorbance readings.

Toxicity Characterization

Cytotoxicity Assay on Caco-2 and HEK 293 Cell Line

As colistin is known to cause severe nephrotoxicity,[26] a cytotoxicity assay was performed on human embryonic kidney cells (HEK 293: ECACC 85120602). Additionally, cytotoxicity toward the human caucasian adenocarcinoma cell line (Caco-2: ECACC 86010202), a common cell line applied in cytotoxicity screenings, was investigated.[14,27,28] Accordingly, cells were seeded in a sterile 96-well cell culture plate in a concentration of 5×10^4 cells per well in a final volume of 100 µL of MEM supplemented with 10% (V/V) heat inactivated FBS and penicillin/streptomycin solution (100 units/0.1 mg/L). The cells were grown for two days at 37 °C in an atmosphere of 95% relative humidity and 5% CO_2 to reach confluency. Samples were prepared in concentrations corresponding to 250, 100, 50, and 10 µg/mL of colistin in a 1:1 mixture of 20 mM HEPES buffer pH 7.4/HEPES-glucose buffer pH 7.4 (Composition: 268 mM glucose, 25 mM HEPES). The same mixture was used as positive control, whereas a Triton X-100 solution 0.1% (m/V) served as negative control. The remaining MEM supernatant was removed and 100 µL of the samples were added to the wells. The samples were incubated for 2 h on the cells at 37 °C. After the incubation period, the supernatant was discarded and 150 µL of 8.8 µM resazurin solution was added and incubated for another 2 h on the cells. Subsequently, 100 µL of the supernatants were transferred to a 96-well fluorescence plate and the fluorescence intensity was measured at an excitation wavelength of 540 nm and an emission wavelength of 590 nm using the Tecan. Cell viability was calculated according to Equation (2):

$$\text{Cell viability}\,(\%) = \frac{\text{intensity of sample} - \text{intensity of negative control}}{\text{intensity of positive control} - \text{intensity of negative control}} x100\% \quad (2)$$

Hemotoxic Potential

The hemotoxic effects of the prepared nanoparticles in comparison with those of free colistin were evaluated by a hemolysis assay.[27] Samples were prepared in concentrations corresponding to 500, 200, 100, and 20 µg/mL of colistin, in 20 mM HEPES buffer pH 7.4. The same buffer served as negative control, while Triton X-100 0.1% (m/V) was used as positive control. Prior to the experiment, erythrocyte concentrate was diluted 1:200 with HEPES-glucose buffer pH 7.4. Next, 500 µL of diluted erythrocytes were mixed with 500 µL of the nanoparticle solution and incubated for 24 h at 100 rpm and 37 °C in a shaking incubator. Subsequently, the samples were centrifuged at 500 × g and 100 µL of the supernatants were added to a 96-well plate. The absorbance was measured at 415 nm. The degree of hemolysis was calculated using Equation (3):

$$\text{Hemolysis}\,(\%) = \frac{\text{absorbance}\,(\text{sample}) - \text{absorbance}\,(\text{negative control})}{\text{absorbance}(\text{positive control}) - \text{absorbance}\,(\text{negative control})} x100\% \quad (3)$$

Microorganisms and Growth Conditions

Two *Micrococcus luteus* strains were isolated from patients undergoing periprosthetic joint infection treatment at the University Hospital for Orthopaedics and Traumatology, Medical University Innsbruck. The protocol used for the isolation of strains was evaluated and approved by the Human Ethics Committee of the Medical University Innsbruck (AN2017-0072 371/4.24,396/5.11–4361A). The study complied with the Declaration of Helsinki. All patients provided informed written consent to take part in the research prior to commencement of the study. The Division of Hygiene and Medical Microbiology Department of the Medical University Innsbruck carried out the identification of all isolates using conventional microbiological cultures, followed by confirmation of bacterial identification using matrix-assisted laser desorption/ionization time-of-flight mass spectrometry (MALDI-TOF-MS) under certification ISO EN 9001–2008.[29,30] After identification, each strain was cryopreserved at −80 °C in special medium until the realization of the tests.[31] At the time of the experiments, the strains were activated by cultivation in TSB medium at 37 °C under shaking. The strains presented differential colony pigmentation (cream-white, identified here as *M. luteus* isolate 1 and yellow, *M. luteus* isolate 2). Glycerol stock solutions of the bacteria were stored at −20 °C until use.

Antimicrobial Activity Determination

The minimum inhibitory concentration (MIC) was estimated by the broth dilution method.[32] Serial 2-fold dilutions of colistin (2 mg/mL), PP (20 mg/mL) and CP-NPs ($c_{Colistin}$ = 500 µg/mL) were prepared in sterile water and added to a 96-well plate containing TSB and 10^5 CFU/mL of *M. luteus* isolates. The blank control consisted of sterile TSB and water, while the growth control involved 10^5 CFU/mL of *M. luteus* isolates in TSB and water. After incubation for 18–21 h at 280 rpm and 37 °C, absorbance at 620 nm was measured. MIC was defined as the lowest antibiotic concentration resulting in no turbidity.[33] From wells showing no turbidity, an aliquot of 100 µL was plated on TSA and incubated for 18 h at 37 °C. The minimum bactericidal concentration (MBC) was defined as the lowest concentration (µg/mL) of antibiotic that reduced the number of bacteria by 99.9% (3 logarithms).[33]

Micrococcus Luteus Biofilm Establishment and Characterization

M. luteus isolates were propagated in TSB incubating overnight for 18–21 h at 37 °C while shaking. The following day, the culture was transferred to TSB and pre-incubated for 1 h at 37 °C with shaking until exponential growth was reached. Then, 10^5 CFU/mL were inoculated using TSB or TSB supplemented with glucose (1%) in a 12-well plate containing 21 glass beads (ColiRollers™ plating beads, Merck) and further incubated for 24 h at 37 °C with shaking.

Determination of Biofilm Composition

In order to estimate the amounts of the three main extracellular polymeric substances in *M. luteus* biofilms, matrix proteins (MPs), extracellular polysaccharides (EPs), and eDNA,[34] biofilms were incubated under mild agitation for 15 min at 37 °C with (I) TrypLE, (II) $NaIO_4$ (0.04 mmol/mL) or (III) DNase I (100 U/mL). The treated samples were stained with 0.1% (m/V) crystal violet and thoroughly washed with demineralized water. Afterward, the bound dye was dissolved in 1 mL of 33% glacial acetic acid. The biomass before and after treatment was determined by photometric measurement at 593 nm.[35]

Quantification of Colony Forming Units

Bacterial harvesting from the 21 glass beads was performed by addition of 1 mL of TrypLE to initiate biofilm disruption. The samples were incubated with TrypLE for 15 min at 37 °C while shaking. Plating of dilutions (10^{-1}–10^{-6}) in TSA was performed after energetic vortexing and CFU were counted after plate incubation for 48 h at 37 °C.

Evaluation of Metabolic Activity

The metabolic activity of the biofilm was determined by photometric measurement at 593 nm as previously reported with some modifications.[35] Biofilms were incubated for 4 h at 37 °C with a 0.3% MTT solution in PBS mixed 1:1 with TSB under shaking. Before absorbance measurement, 1 mL of dimethyl sulfoxide (DMSO) was added to extract the formazan product produced after the reduction of MTT by the bacteria.

Quantification of AP Activity

AP activity was quantified colorimetrically after hydrolysis of the AP substrate p-nitrophenyl phosphate (5 mM) in a buffer containing $MgCl_2$ (5 µM) and 2-amino-2-methyl-1-propanol (500 mM). *M. luteus* biofilms and planktonic cells were washed three times with PBS and incubated for 1 h at 37 °C with the AP substrate. Absorbance was measured at 450 nm and activity was determined using a calibration curve obtained with different concentrations of AP.

Effect of CP-NPs and Colistin on Bacterial Biofilm

Biofilms of *M. luteus* isolates 1 and 2 were obtained separately as described in Section 2.8. After 3 washing steps with PBS to remove planktonic bacteria, the biofilms were treated with HEPES buffer pH 7.4 (negative control), colistin (500 µg/mL) or CP-NPs ($c_{Colistin}$ = 500 µg/mL) for one day at 37 °C. Biofilm characterization was performed after sample removal and rinsing thrice with PBS as described above.

Furthermore, to gain insight into the kinetics of killing in a mixed biofilm, *M. luteus* isolates 1 and 2 were co-cultured and the obtained biofilm was treated with HEPES buffer pH 7.4 (negative control), colistin (500 µg/mL) or CP-NPs ($c_{Colistin}$ = 500 µg/mL). Biofilm characterization after treatment was performed at predetermined time points over

a period of seven days. Additionally, the *M. luteus* biofilms grown on glass beads before and after treatment were morphologically characterized using SEM. Thus, samples were fixed for 24 h at 4 °C in 2 mL of glutaraldehyde 2.5%. After fixation, the samples were dehydrated using an ascending alcohol series (50%–70%–80%–99.9% ethanol). Each step lasted 5 min. The dried samples were mounted on aluminum pins with Leit-C glue. The pins were sputtered with Au using an automatic sputter coater (Agar Scientific Ltd., Stansted, UK) for 45s and analyzed by scanning electron microscopy (SEM, JSM-6010LV, JEOL GmbH, Freising, Germany).[36]

Statistical Data Analysis

Statistical data analysis was performed using one-way ANOVA in combination with Bonferroni post-hoc-test to analyze the significance of differences between the means of more than two groups calculated with GraphPad Prism 5.01, while Student's *t*-test was used to compare the means of two groups. The level of $p < 0.05$ was set as the minimum level of significance.

Results and Discussion

Characterization of Colistin-Polyphosphate Nanocomplexes

Preliminary experiments were carried out to determine the appropriate concentration range as well as the ratio of colistin: polyphosphate (COL:PP), which leads to the formation of nanoparticles (data not shown). On the one hand, it was found that the concentration of colistin should not exceed 1 mg/mL, while, on the other hand, the concentration of PP has to be at least 0.4 mg/mL to form complexes in the nanometer range. Whenever these requirements were not met, large macroscopic agglomerates were obtained instead of a slightly turbid solution. Results of particle characterization are presented in Table 1.

Table 1 Size, PDI and Zeta Potential of CP-NPs Formed by Ionic Gelation in Indicated Media. Data are Means (n=3) ± Standard Deviation

Ratio COL:PP	Size (nm)	PDI	Zeta potential (mV)
HEPES 20 mM, pH 6.8			
1:0.4	135.1 ± 4.3	0.17 ± 0.02	−39.4 ± 1.1
1:0.6	127.2 ± 1.9	0.17 ± 0.01	−42.0 ± 1.1
1:0.8	137.2 ± 18.0	0.25 ± 0.05	−43.3 ± 4.0
HEPES 20 mM, pH 7.4			
1:0.4	170.3 ± 9.4	0.12 ± 0.01	−29.2 ± 0.8
1:0.6	128.4 ± 3.8	0.17 ± 0.01	−38.5 ± 1.1
1:0.8	122.8 ± 8.3	0.20 ± 0.04	−41.7 ± 0.6
Demineralized Water			
1:0.4	155.8 ± 5.5	0.14 ± 0.02	−41.5 ± 0.4
1:0.6	152.7 ± 3.7	0.23 ± 0.02	−48.3 ± 2.3
1:0.8	141.0 ± 3.8	0.19 ± 0.02	−52.0 ± 2.1
0.01 M HCl			
1:0.4	Precipitation		
1:0.6	172.4 ± 14.2	0.16 ± 0.01	−29.9 ± 0.4
1:0.8	157.2 ± 2.8	0.15 ± 0.00	−36.8 ± 0.1

CP-NPs formation was successful in various aqueous media and pH conditions except for 0.4 mg/mL PP in 0.01 M HCl, for which precipitation due to agglomerate formation was observed. This is likely due to pronounced electrostatic interactions, as colistin exhibits more positive charges at low pH than at neutral pH conditions. In all other cases, appropriate particle sizes in the nanometer range were obtained, which can be a crucial factor for the antimicrobial performance of nanomaterials.[1] No major differences in particle size, PDI or zeta potential were found for the different colistin to polyphosphate ratios, as listed in Table 1. EFTEM images of the developed colistin-polyphosphate nanocomplexes are shown in Figure 1, confirming the formation of round, spherical nanoparticles.

To ensure consistency in the following experiments, the concentrations of the solutions used to prepare the nanoparticles were fixed to 1 mg/mL for colistin and 0.4 mg/mL for PP in 20 mM HEPES buffer pH 7.4. The colistin complexation efficiency for this nanoparticle formulation was determined to be >95%. Accordingly, the final concentrations of colistin and PP in the nanoparticle stock solution were 500 µg/mL and 200 µg/mL, respectively.

AP-Triggered Change in Size and Zeta Potential

Changes in size and zeta potential of the nanoparticle formulation were evaluated for AP concentrations of 0.2 U/mL and 0.02 U/mL, which is in a common concentration range described in literature for experiments with isolated AP.[11,37] As depicted in Figure 2, incubation of CP-NPs with AP in concentrations of 0.2 U/mL as well as 0.02 U/mL led to a time-dependent shift in zeta potential to more positive values as well as an increase in size over 24 h. Due to the activity of the enzyme, anionic monophosphate groups are cleaved off the polyphosphate structures, thereby reducing the anionic charge of the particles. Subsequently, the electrostatic repulsion decreases, favoring instability and an increase in particle size due to agglomeration.[37] Indeed, after seven days of incubation, macroscopic agglomerates were visible in the samples containing AP and were thus not subjected to further size, PDI and zeta potential measurements.

An enzyme concentration of 0.2 U/mL of AP caused an increase in the zeta potential of the particles of approximately +12 mV within just 2 h. Afterward, the zeta potential remained almost constant until the 24 h time point, while the size continuously increased from initially 170 nm to approximately 360 nm. The change in zeta potential observed for 0.02 U/mL was comparatively slower, reaching a total increase of approximately +10 mV after 24 h of incubation. Moreover, the corresponding change in size was not as apparent as that observed for the higher concentration of AP. In contrast, the control particles, which were incubated without AP, showed no significant changes in physical parameters over 24 h.

Enzyme-Triggered Release Kinetics

As polyphosphate nanoparticles can be cleaved by AP, the time-dependent release of monophosphate and colistin from the nanoparticles was investigated in the presence and absence of the enzyme. The malachite green assay was used to quantify the amount of inorganic monophosphate cleaved off the CP-NPs in the presence of 0.2 U/mL or 0.02 U/mL of AP. The

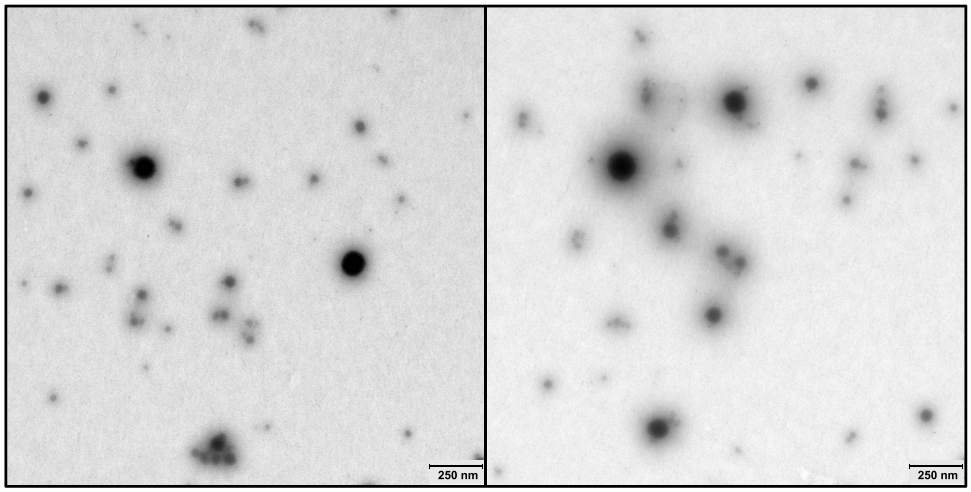

Figure 1 EFTEM images of CP-NPs in a dilution of 1:10 in water.

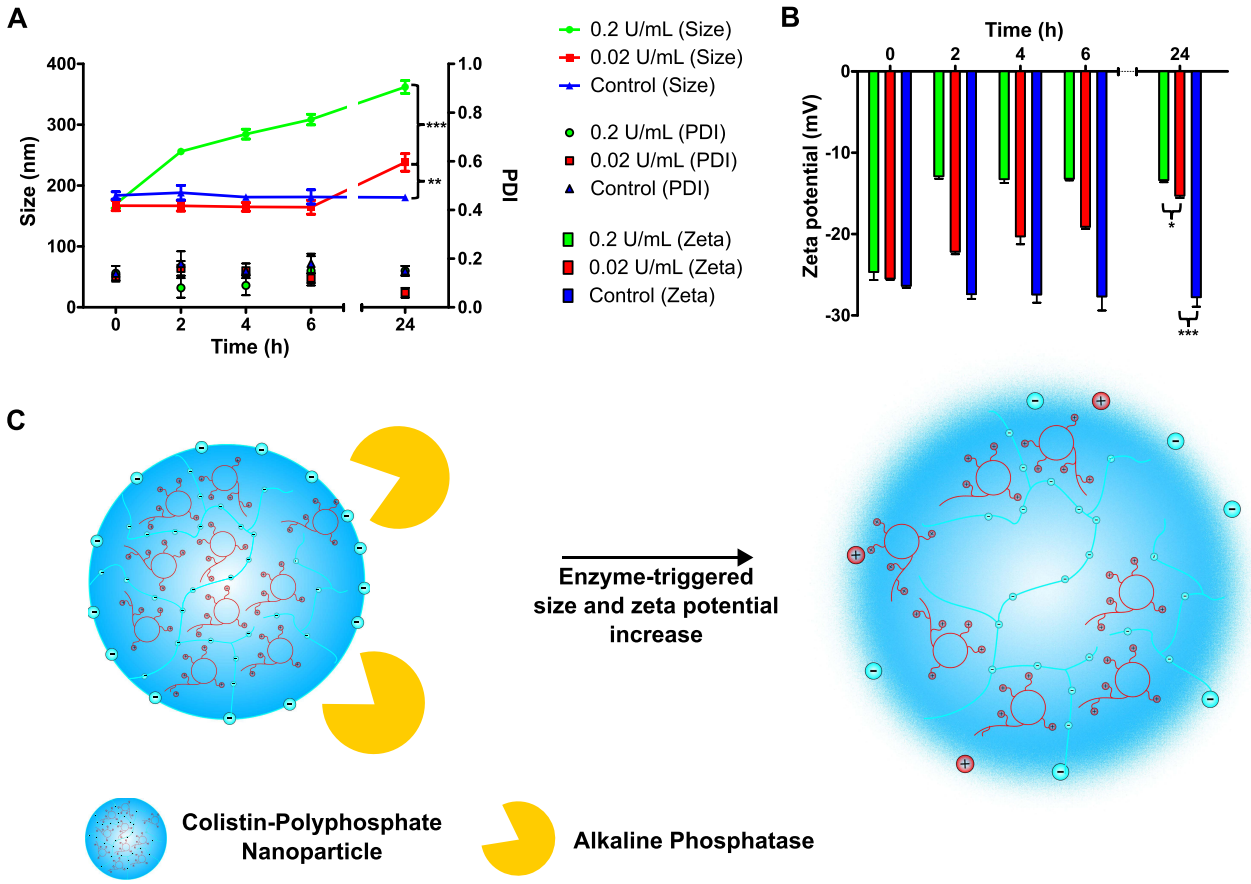

Figure 2 Size, PDI (**A**) and zeta potential (**B**) of CP-NPs in 20 mM HEPES buffer pH 7.4 over 24 h in the presence of 0.2 U/mL (green) or 0.02 U/mL (red) of AP. The negative control (blue) was performed in the absence of AP. Data are means (n=3) ± standard deviation. Significant differences compared to the control are indicated as *p<0.05, **p<0.01, ***p<0.001. Schematic representation of AP-triggered increase in size and zeta potential of CP-NPs (**C**).

negative control contained just the nanoparticles without AP. The results of the phosphate release study are illustrated in Figure 3A. While 0.2 U/mL AP led to an overall higher release of inorganic phosphate compared to 0.02 U/mL AP, similarly shaped release profiles were observed for both concentrations of AP. After three days of incubation, the phosphate concentration remained almost constant. This plateau has already been observed in previous studies[14,38] and might be the result of feedback inhibition of AP by the presence of high concentrations of inorganic phosphate in the experimental setup.[39] However, in an in vivo situation, inorganic phosphate is constantly eliminated and enzyme activity could therefore resume. The negative control showed no significant release of phosphate over seven days, indicating stability of the CP-NPs toward non-specific hydrolysis.

In order to verify, that the cleavage of polyphosphate leads to a subsequent release of colistin from the CP-NPs, a drug release study with 0.2 U/mL and 0.02 U/mL of AP via dialysis setup was carried out. Colistin complexed in the nanoparticle formulation cannot permeate the dialysis membrane, whereas free colistin is sufficiently small to permeate the pores of the membrane (cut-off: 300 kDa). As an additional control, free colistin solution was tested to evaluate a possible impact of the dialysis membrane on the release kinetics. As shown in Figure 3B, free colistin was immediately released from the dialysis tube, reaching a maximum concentration after 24 h. The measured value is equal to 80% of the calculated theoretical maximum release. After that, the colistin concentration was slightly, but gradually decreasing. This can be attributed to two main factors: (I) Colistin is a peptide showing minor long-term stability in buffered solutions at 37 °C.[40] Thus, the observed decrease in concentration could have been caused by degradation. (II) There is evidence that colistin binds to plastics,[41] which is the material used in the dialysis and the Falcon tubes. Due to these limitations, a prolonged incubation period to reach 100% release was not reasonable in this case. Hence, the experiment was stopped after seven days of incubation. The CP-NPs incubated with either 0.2 U/mL or 0.02 U/mL AP showed an almost linear release of colistin over seven days which is in good

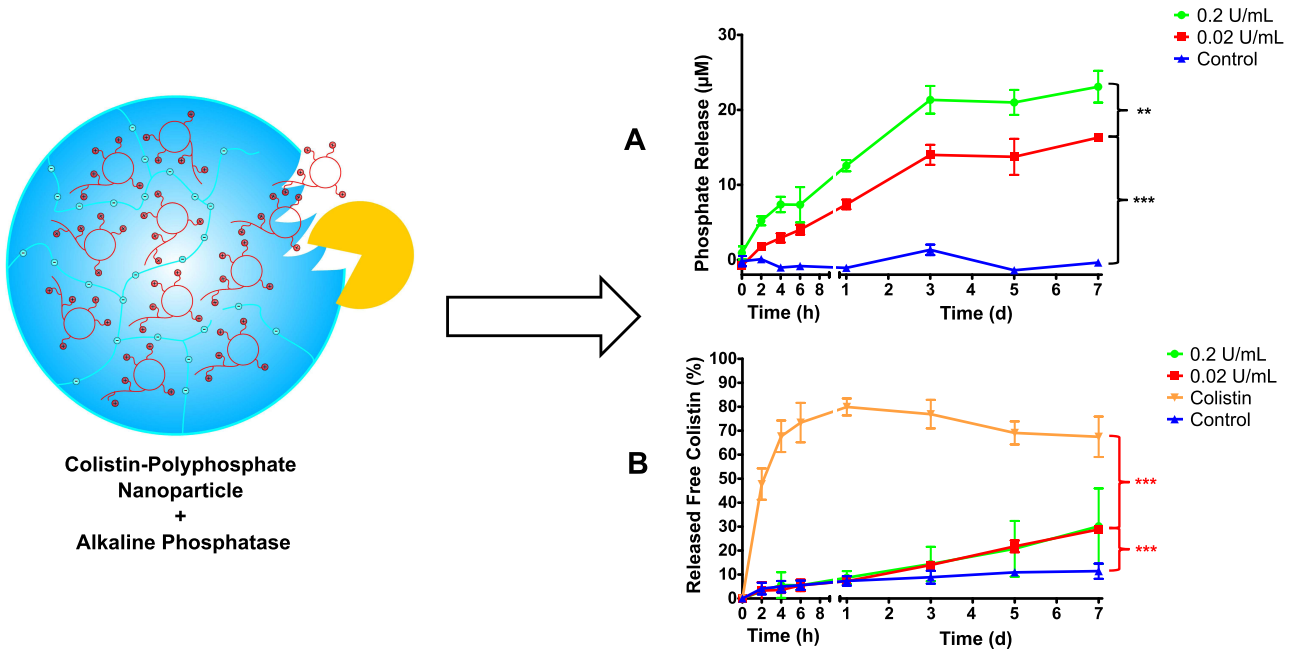

Figure 3 Release kinetics from CP-NPs: Monophosphate release (**A**), colistin release (**B**) over seven days in the presence of 0.2 U/mL (green circles) or 0.02 U/mL (red squares) of AP. The negative control (blue triangles) was performed with CP-NPs in the absence of AP. Colistin solution (Orange inverted triangles) served as additional control for drug release. Data are means (A: n=3; B: n≥3) ± standard deviation. Significant differences are indicated as **p<0.01, ***p<0.001.

agreement with the results obtained by Hock et al for their nanoparticle formulation based on amikacin and polyphosphate.[11] However, there was no significant difference in the amount of colistin released between the two AP concentrations tested. For both cases, the mean concentration measured at day 7 corresponded to a release of approximately 30% of previously complexed colistin, compared to roughly 10% for the control particles without AP. This is again in line with the release kinetics of the polyphosphate nanoparticles described by Hock et al.[11] As colistin has to be administered repeatedly over a period of at least several days up to more than a month to treat bacterial infections in a clinical setting,[42–44] and even sub-minimum inhibitory concentrations of colistin are known to possess anti-biofilm effects,[45] the observed release kinetics appear to be highly favorable for the eradication of persistent bacterial biofilms. Based on the data obtained, we conclude that there is an AP-triggered release of colistin from CP-NPs. A comparatively low concentration of 0.02 U/mL of AP was in our experimental model already sufficient to induce colistin release from CP-NPs.

Characterization of Toxicity

The results of the cytotoxicity screening are depicted in Figure 4. Generally, colistin as well as CP-NPs were well tolerated within the investigated concentration range, with resulting cell viabilities >90% (Caco-2, A) and >75% (HEK 293, B). However, at a concentration of 100 µg/mL (HEK 293) and 250 µg/mL (Caco-2), slight, but significant decreases in cell viability were observed for the free colistin solution in comparison to the nanoparticle formulation. A possible explanation for this observation might be the polycationic nature of colistin, which interferes with the anionic charged cell membrane, thereby causing cell disruption.[46] By complexing colistin with PP, the polycationic character is partially masked, potentially resulting in reduced interference with the cell membrane. Different toxicity profiles comparing CP-NPs and colistin were more apparent in the investigation of hemotoxicity as shown in Figure 4C.

Under the test conditions, all concentrations of colistin resulted in ≥40% of hemolysis compared to the 100% control, whereas CP-NPs exhibited ≤10% of hemolysis at all tested concentrations after 24 h of incubation. The difference between the two samples was distinct and more apparent than that observed in cytotoxicity assays. The interaction of xenobiotics with the erythrocyte membrane causes an extracellular release of hemoglobin, indicating cellular damage.[47] These results therefore highlight the impact of membrane interactions for the cytotoxicity of colistin. Complexation with PP appears to limit interference with the cell membrane, thereby reducing hemotoxicity of colistin.

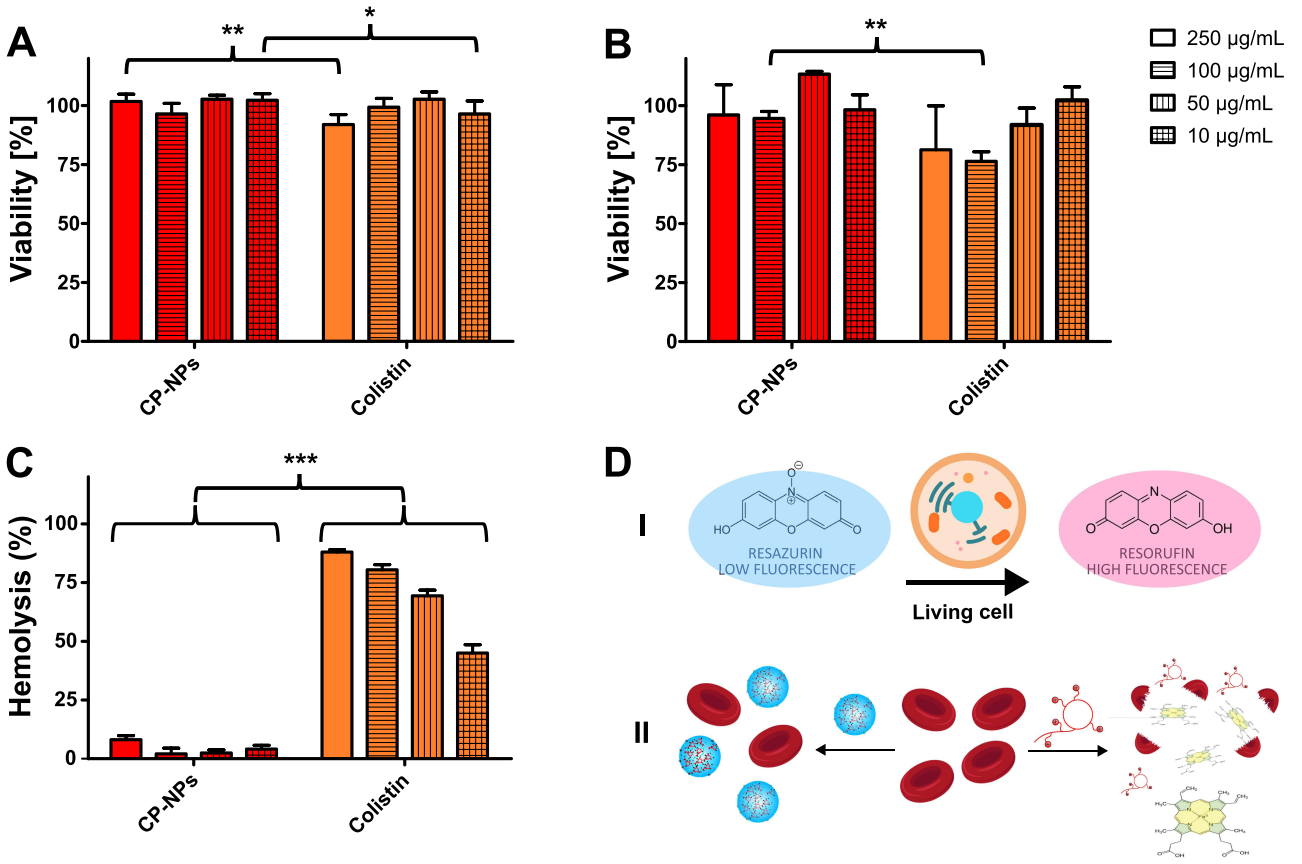

Figure 4 Cytotoxicity of CP-NPs and colistin on Caco-2 cell line (**A**) and HEK-293 cell line (**B**) after 2 h of incubation, as well as hemolysis (**C**) after 24 h of incubation in the concentrations 250 µg/mL (blank bars), 100 µg/mL (horizonal striped bars), 50 µg/mL (vertical striped bars) and 10 µg/mL (grid bars). Data are means (A: n≥3; B: n≥3; C: n=4) ± standard deviation. Significant differences are indicated as *p<0.05, **p<0.01, ***p<0.001. Schematic representation of the principles of cytotoxicity assays (**D**): resazurin (I) and hemolysis (II).

Effects of Colistin and CP-NPs on M. Luteus

Antibacterial Effect on Planktonic M. Luteus

Colistin, PP and CP-NPs MIC and MBC were preliminarily determined against *M. luteus* isolates 1 and 2 planktonic cells by microbroth dilution and subsequent plating. The results are shown in Table 2.

Although isolate 1 was sensitive to colistin (MIC and MBC of 7.8 µg/mL), CP-NPs showed no antimicrobial effect at the assessed concentration (250 µg/mL). In contrast, *M. luteus* isolate 2 was resistant to colistin (MIC >1000 µg/mL) and showed also no sensitivity to CP-NPs (MIC >250 µg/mL). Interestingly, the cells were not culturable after exposure to colistin, which is regarded as a mechanism of survival that increases antibiotic tolerance and resistance.[48]

Table 2 Colistin and CP-NPs MIC and MBC Against Planktonic Bacteria. Data are Means (n=6)

Sample	*M. luteus* Isolate 1		*M. luteus* Isolate 2		*M. luteus* Co-Culture	
	MIC (µg/mL)	MBC (µg/mL)	MIC (µg/mL)	MBC (µg/mL)	MIC (µg/mL)	MBC (µg/mL)
Colistin	7.8	7.8	Higher than 1000	ND	125	125
PP	Equal or higher than 1250	Not found: Bacteriostatic	Equal or higher than 1250	Not found: Bacteriostatic	Equal or higher than 1250	Not found: Bacteriostatic
CP-NPs	Higher than 250*	Higher than 250*	Higher than 250*	Higher than 250*	Higher than 250*	Higher than 250*

Notes: *250 µg/mL colistin was the highest concentration that could be assessed by this method. ND, cells were not culturable after exposure to the antibiotic at the assayed concentrations.

However, when a mixed culture of both isolates was assessed for MIC, 125 µg/mL of colistin was sufficient to kill planktonic bacteria, while CP-NPs again showed no antibacterial effect. These results highlight once more that even though colistin has high efficacy against gram-negative bacterial germs,[16] it also possesses activity against certain gram-positive microorganisms, such as *M. luteus* and could therefore be useful in associated infections. The observation that CP-NPs were not effective in any of the three cases suggests that the nanoparticles themselves have only minor antimicrobial activity, as the complexed colistin cannot exert its antibacterial effect. Colistin's mode of action involves electrostatic interactions with the bacterial cell,[46] which are mediated by the cationic amine groups. As the cationic charges are covered with polyphosphate in CP-NPs, complexed colistin cannot interact with the bacterial cell. While bacteriostatic properties were found for polyphosphate solution on all tested strains (MIC ≥1250 µg/mL), no bactericidal activity was observed, and the determined MIC values were more than 12 times higher than the PP concentrations incorporated in the tested CP-NPs ($c_{Colistin}$ ≤250 µg/mL, c_{PP} ≤100 µg/mL). The MIC values found for PP are in good agreement with values reported by Lorencová et al.[49] Conclusively, CP-NPs presented no antimicrobial effect, as solely free colistin is able to exert antimicrobial effects on planktonic *M. luteus* in the investigated concentration range. As described in section 3.3, the presence of sufficient AP activity is required for the dissociation of CP-NPs, causing release of the active antibiotic colistin and thereby triggering the antimicrobial effect. Quantification of AP activity in planktonic *M. luteus* pellets revealed a negligible AP activity of around 0.00025 U/Log (CFU) (Supplementary materials Figure S1), which is in good agreement with the absence of an antimicrobial effect of CP-NPs in this case.

Nonetheless, experiments on bacteria in the planktonic state can only serve as a preliminary indicator of the antibacterial performance of a material, as persistent bacterial infections typically involve biofilm formation.[2]

Investigations on M. Luteus After Biofilm Formation

TSB supplemented with 1% glucose was selected as growth medium for *M. luteus*, as this led to the formation of bacterial biofilms with high biomass (Supplementary materials Figure S2). An initial screening on the AP activity of *M. luteus* biofilm revealed a more than 25-fold increase in AP activity compared with the planktonic state, resulting in a corresponding AP activity of around 0.0064 U/Log (CFU) (Supplementary materials Figure S1). This means that *M. luteus* in biofilm state expresses significantly higher AP activity than in planktonic state, independently of the cell number reached after growth. Therefore, bacterial biofilms appear to be a more suitable target for CP-NPs than planktonic cells.

The established biofilms were further characterized regarding their composition, and the results are shown in Figure 5A and B. The biofilms were treated with different agents which are known to degrade specific components of the biofilm matrix, namely TrypLE (MPs), $NaIO_4$ (EPs), and DNase I (eDNA). A distinct decrease in absorbance at 593 nm after crystal violet staining thus indicates the presence of high amounts of the degraded compound in the initial biofilm.

After treatment with TrypLE, a strong biomass reduction was observed for both analyzed isolates, suggesting a biofilm matrix mainly composed of proteins, with lower contributions of EPs and eDNA. The composition of the extracellular polymer matrix in bacterial biofilms is highly diverse, depending on host conditions, nutritional values as well as external physical stress.[1] *M. luteus* biofilm composition reported in the literature is dependent on biofilm maturity and the conditions under which the biofilm was obtained. It is generally showing different results for different isolates.[34,50] Similarly, the composition of the mixed biofilm obtained by co-culturing *M. luteus* isolates 1 and 2 was analyzed and the results are depicted in Figure 5B. An increased content of eDNA and MPs was observed compared with the amounts of EPs. SEM analyses showed that intercellular connections between bacteria seemed to be removed after TrypLE treatment (II) compared to $NaIO_4$ (III) or DNase I treatment (IV).

Time-Kill Assays on M. Luteus Biofilm

Colony counts and AP activity after the characterized biofilms of *M. luteus* isolates 1 and 2 were treated with HEPES buffer pH 7.4, colistin and CP-NPs are shown in Figure 6A and B, respectively.

Colistin reduced the number of CFU in both isolates. However, the efficacy in eradicating biofilms formed by isolate 2 was less pronounced, which is in good agreement with the results of the MIC/MBC determination. No statistically

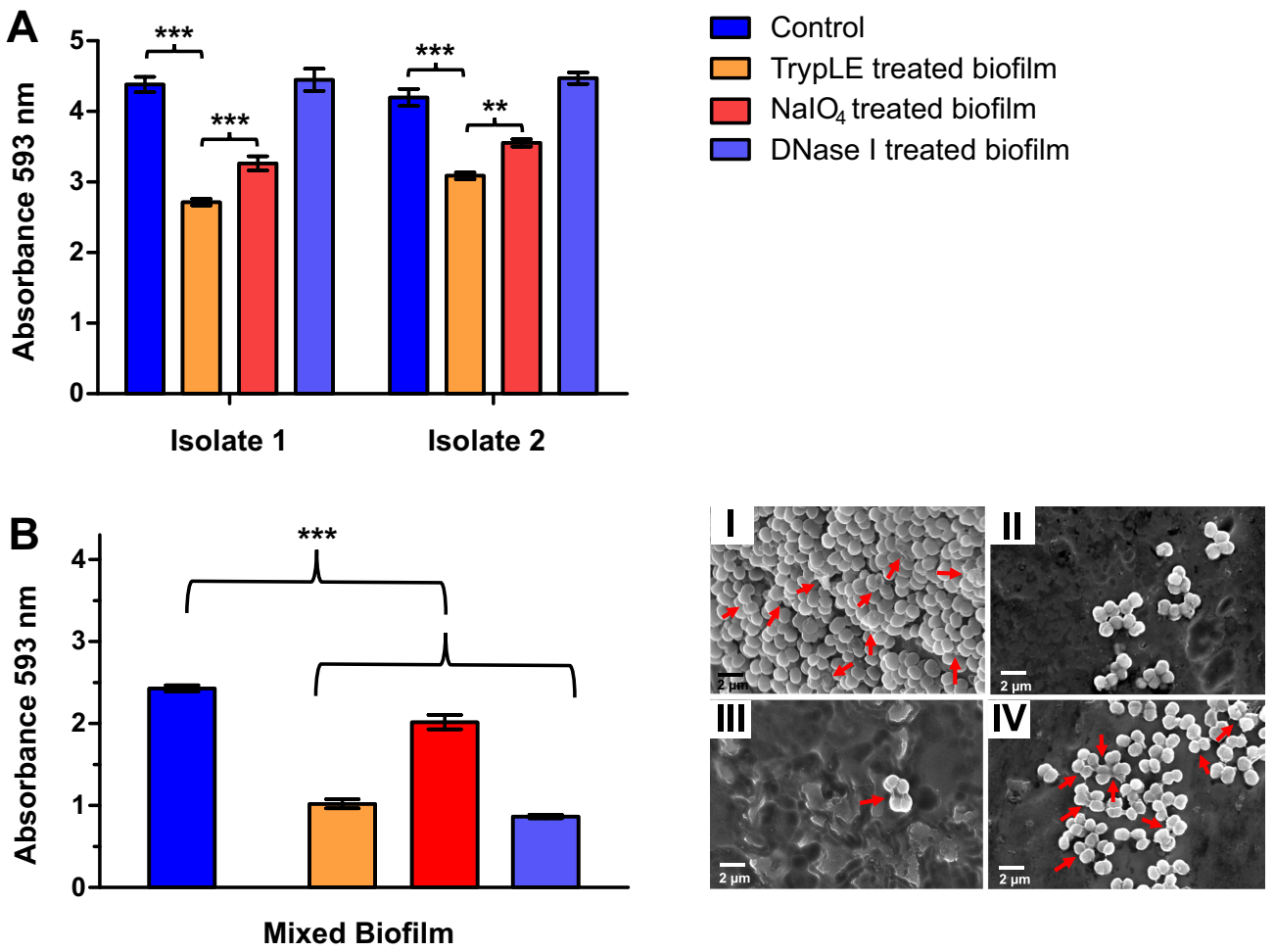

Figure 5 Biofilm characterization of *M. luteus* isolate 1 and 2 (**A**) and mixed *M. luteus* biofilm (**B**) before (dark blue, I) and after treatment with TrypLE (Orange, II, degrades MPs), NaIO4 (red, III, degrades EPs) and DNase I (light blue, IV, degrades eDNA). Arrows show cells interconnected by slime-like substances. A significant decrease in absorbance after treatment with the respective degrading agent correlates with a high amount of the degraded compound in the initial biofilm. Data are means (n=3) ± standard deviation. Significant differences compared to the control are indicated as **p<0.01, ***p<0.001.

significant changes in AP activity were observed upon treatment with colistin or CP-NPs. Despite the fact that CP-NPs were completely ineffective against planktonic *M. luteus*, significant reductions in CFU were also observed for samples treated with the nanoparticle formulation. This could be a result of strongly increased AP levels after biofilm formation, as described above. Accordingly, we hypothesized that given a residual enzymatic activity, longer treatments of *M. luteus* biofilms will lead to a higher effectiveness of CP-NPs, mimicking a persistent infection with bacterial biofilm. To test this hypothesis, we performed a time-kill assay over seven days in a mixed biofilm composed of both isolates of *M. luteus*.

As illustrated in Figure 7A, the biofilm initially presented an initial AP activity around 0.02 U and the typical structural features of a biofilm in a maturation phase[51] which are depicted in Figure 7B.

On the first day of incubation with HEPES buffer 7.4, colistin and CP-NPs, AP activity was significantly higher in the biofilm incubated with CP-NPs compared to the control and colistin. The physiological function of AP is to supply inorganic phosphate (P_i) from polyphosphate substrates. Literature suggests that in some species of staphylococci, this enzyme is constitutively expressed, whereas in other bacteria such as *E. coli* and *M. luteus*, the level of expression of AP is regulated by the cellular levels of P_i, being repressed in the presence of P_i and activated in the absence of P_i.[23,39] However, the effect of polyphosphate substrates on the production of AP by biofilms has not been discussed. In our study, the increased AP expression in the presence of CP-NPs likely impacted positively on the antimicrobial efficacy after five days of incubation, in which CP-NPs reached higher biofilm eradication than colistin. Sufficiently high AP activity is a prerequisite for inducing colistin release from CP-NPs, subsequently resulting in an antimicrobial effect, as

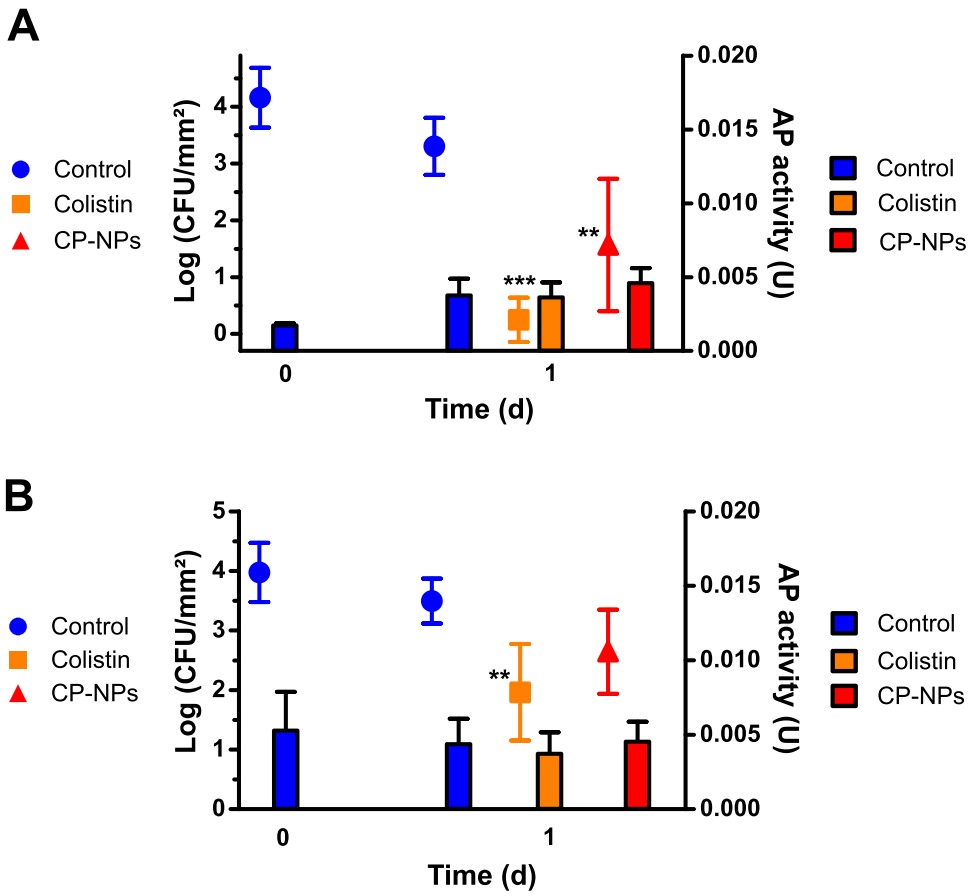

Figure 6 Colony counts (bars) and AP activity (dots) in biofilm formed by *M. luteus* isolate 1 (**A**) and *M. luteus* isolate 2 (**B**) after treatment with HEPES buffer pH 7.4 (negative control, blue bars, blue circles), colistin ($c_{Colistin}$ = 500 µg/mL, Orange bars, orange squares) and CP-NPs ($c_{Colistin}$ = 500 µg/mL, red bars, red triangles) for one day. Data are means (CFU: n=6; AP: n=9) ± standard deviation. Significant differences compared to the negative control of day 1 are indicated as **p<0.01, ***p<0.001.

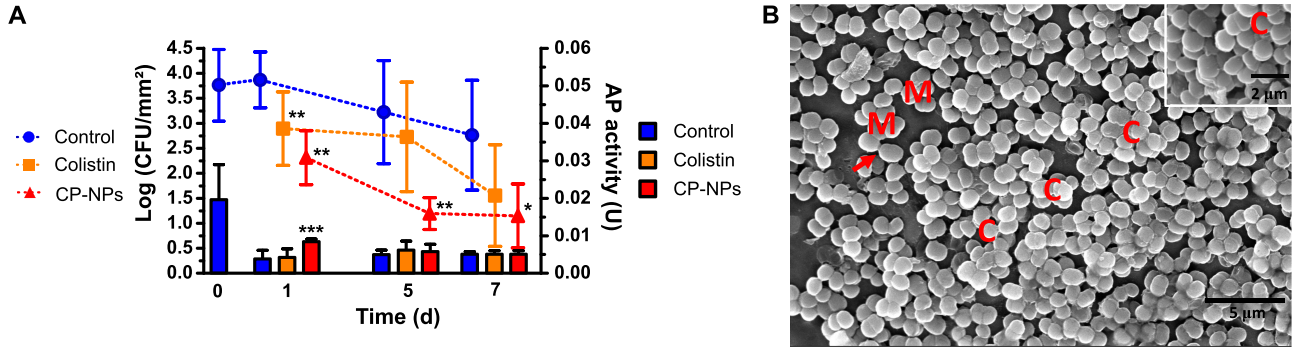

Figure 7 Colony counts (bars) and AP activity (dots) over seven days in the presence of HEPES buffer pH 7.4 (negative control, blue bars, blue circles), colistin ($c_{Colistin}$ = 500 µg/mL, Orange bars, orange squares) and CP-NPs ($c_{Colistin}$ = 500 µg/mL, red bars, red triangles) (**A**). Data are means (CFU: n=6; AP: n=9) ± standard deviation. Significant differences compared to the negative control are indicated as *p<0.05, **p<0.01, ***p<0.001. SEM of *M. luteus* mixed biofilm highlighting features of biofilm according to[51] (**B**). M: micro-colony; C: column; arrows show cells interconnected by slime-like substances.

described above. Differential effectiveness of colistin and CP-NPs is also mirrored by SEM analyses (Figure 8, supplementary materials Figure S3). Microscopy images revealed dispersed biofilms after treatment with colistin and CP-NPs. However, typical structural biofilm features, such as the presence of microcolonies, columns, and slime-like substances, were observed for colistin and the control on day 1, in contrast to CP-NPs treated samples, for which strong morphological changes in the biofilm structure and bacteria were observed.

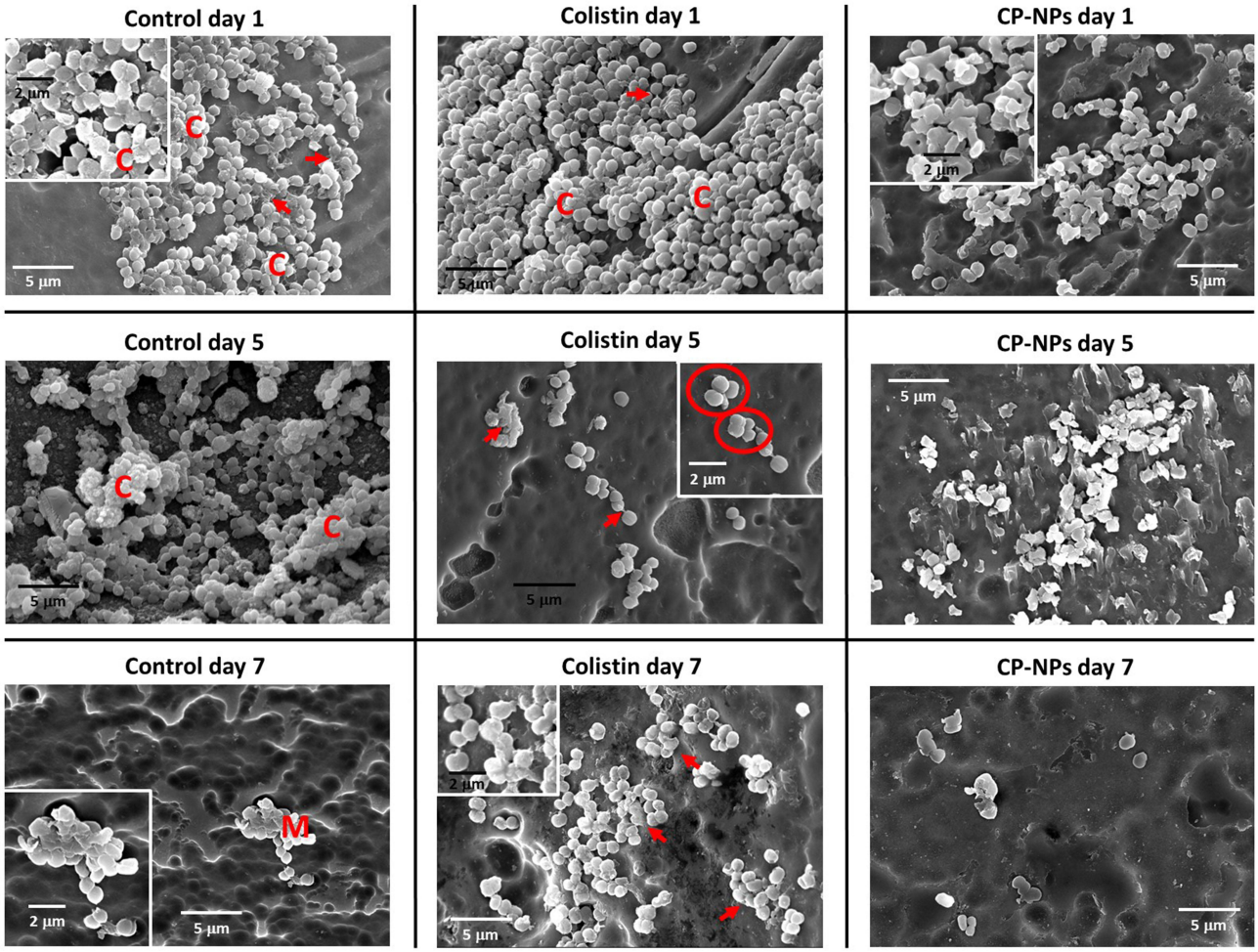

Figure 8 SEM images of *M. luteus* mixed biofilm obtained as a function of treatments and times. M: microcolonies; C: columns; circles highlight initial adhesion features; arrows indicate cells interconnected by slime-like substances.

This indicated decreased viability of biofilms treated with CP-NPs compared to colistin-treated biofilm and control. An additional factor that may be responsible for the efficacy of CP-NPs on bacterial biofilm, aside from the significantly increased AP activity, is likely an altered diffusion profile of the nanoparticle inside this slime-like matrix. Native colistin is polycationic and therefore prone to electrostatic interactions with anionic compounds of the biofilm matrix, such as eDNA, that was found to a large extent in mixed *M. luteus* biofilms (section 3.5.2). This may result in restricted penetration of the polycation inside the biofilm as previously described.[4,13,52] On the other hand, polyphosphate-coacervate nanocarriers exhibit altered diffusion profiles due to different particle size and their anionic surface charge mediated by polyphosphate coverage. This results in a reduced interference of anionic biofilm matrix compounds, thereby favoring antibiotic penetration, as previously reported by our research group.[13] Accordingly, CP-NPs are diffusing freely inside the biofilm, subsequently releasing the complexed colistin after cleavage by present AP. Interestingly, the CFU count decreased after treatment with CP-NPs, but also for treatment with colistin. Considering the high amount of bacterial biofilm detected in the SEM images of samples treated with colistin, it may be suggested that the application of colistin again induced the presence of viable but not culturable bacteria,[48] which was also observed for planktonic *M. luteus* isolate 2 (Table 2).

After five days of incubation, the colistin-treated biofilm appeared to start the adhesion process, which is highlighted by the presence of putative adhesive structures depicted in Figure 8. Further, we observed extracellular slime-like structures interconnecting the cells on day 7, possibly indicating re-colonization of the surface. In contrast, in the samples treated with CP-NPs, only a small number of surviving bacteria was visible and most of them exhibited significant morphological damage.

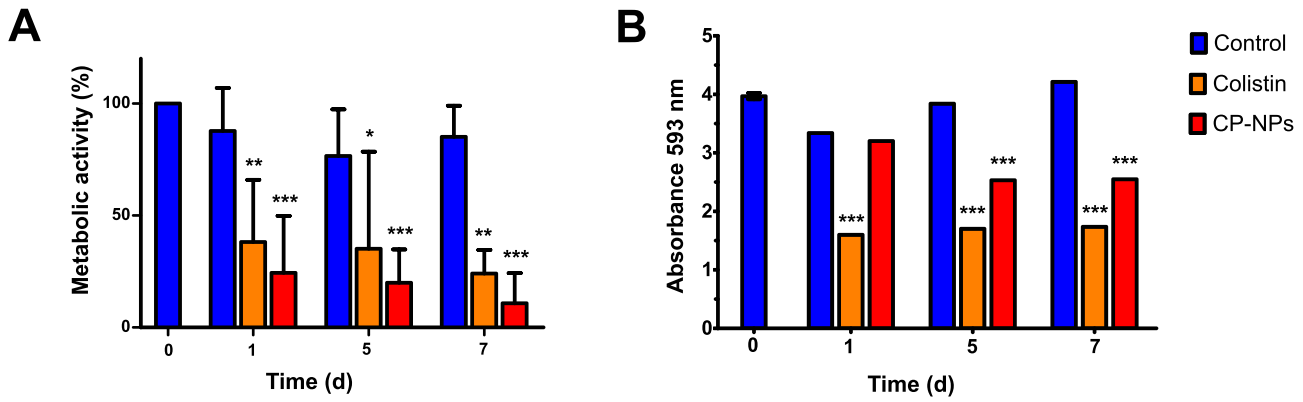

Figure 9 Metabolic activity (**A**) and biomass (**B**) over seven days in the presence of HEPES buffer pH 7.4 (negative control, blue), colistin ($c_{Colistin}$ = 500 µg/mL, Orange) and CP-NPs ($c_{Colistin}$ = 500 µg/mL, red). Data are means (A: n=9; B: n=3) ± standard deviation. Significant differences compared to the respective negative control are indicated as *p<0.05, **p<0.01, ***p<0.001.

In agreement with the cell counts and SEM images, a greater decrease in metabolic activity with respect to the control was observed in the bacteria after treatment with CP-NPs compared to colistin as depicted in Figure 9A. However, according to the analyses of biomass, which are visualized in Figure 9B, the dispersal of extracellular structures by colistin seemed to be higher than that of CP-NPs.

Conclusion

To the best of our knowledge, this study demonstrated the formation of nanoparticles by the complexation of colistin with polyphosphate via ionic gelation for the first time. Previously published nanoparticular formulations for the drug colistin mainly focused on improving the safety profile of colistin[53,54] and on enhancing the antibacterial effectiveness by combining with complementary materials such as silver nanoparticles[54] or chitosan.[55] Accordingly, our developed polyphosphate-based formulation aligns well with the reasonable strategy of applying auxiliary agents to enhance efficacy of conventional antibiotics. The major strength of polyphosphate-coacervate nanocarriers described in literature is endowing AP-triggered release,[10,11] which is a concept that has not been investigated so far for the enhanced eradication of bacterial biofilms. Furthermore, the fabrication of this type of nanocarrier is simple, and no additional expensive equipment or assisting material is required.

CP-NPs showed a mean particle size of <200 nm, narrow particle size distribution and negative zeta potential. Toxicity assessment revealed slightly decreased cytotoxicity toward the human cell lines Caco-2 and HEK-293, as well as significantly reduced hemolytic activity, compared to native colistin. The developed nanoparticles showed responsiveness to AP, subsequently releasing significant amounts of monophosphate and colistin, whereas in the absence of AP only minor release was detected.

CP-NPs were shown to be ineffective against different isolates of the model organism *M. luteus* in planktonic state. As native colistin, in contrast, exhibited antimicrobial activity against planktonic *M. luteus*, the low efficacy of CP-NPs may be attributed to the tremendously low AP activity found in the planktonic pellets, potentially resulting in insufficient drug release.

On the other hand, CP-NPs demonstrated increased efficacy against *M. luteus* after biofilm formation, leading to biofilm disruption, impairing bacterial growth and surface re-colonization when compared to free colistin. A more than 25-fold increase in AP activity compared to the planktonic culture was observed for the biofilm state of *M. luteus*, which could be a key factor for the high efficacy of CP-NPs on bacterial biofilms. To date, no comparable study has provided detailed investigations on the viability of bacterial biofilms after interaction with antibiotic-polyphosphate nanoparticles.

However, as AP is an enzyme that can not only be found in bacteria, but also in certain tissues of the human body,[15] a potential use of this system is currently restricted solely to local applications. Future work should therefore focus on expanding our knowledge on bacterial biofilms by identifying other specific biofilm characteristics, similar to the increased AP activity levels, and exploit them for enhancing selectivity and efficacy of the nanocomplexes that were developed in this work. A promising strategy in this regard might be the application of an additional functional coating, which could be

electrostatically bound to the CP-NPs, similar to the "Layer-by-Layer" approach described by Akkus et al.[56] Given the era of "classic" antibiotics is coming to an end, antibiotic-polyphosphate coacervation represents an innovative tool to tackle bacterial biofilm and yields great potential for the treatment of complicated and persistent infections with microbial biofilm.

Data Sharing Statement

The data that support the findings of this study are available upon request.

Acknowledgments

Dr. Mariana Blanco Massani acknowledges the support of the European Union's Horizon 2020 Research and Innovation Program under Marie Skłodowska-Curie IF [NanoBioRS-101025065].

The authors would like to acknowledge MSc Stephan Josef Maria Steixner (Division of Hygiene and Medical Microbiology, Medical University of Innsbruck, Innsbruck, Austria) for performing MALDI-TOF analyses.

Author Contributions

All authors made a significant contribution to the work reported, whether that is in the conception, study design, execution, acquisition of data, analysis and interpretation, or in all these areas; took part in drafting, revising or critically reviewing the article; gave final approval of the version to be published; have agreed on the journal to which the article has been submitted; and agree to be accountable for all aspects of the work.

Disclosure

The authors declare that they have no known competing financial interests or personal relationships that could influence the work reported in this study.

References

1. Ma R, Hu X, Zhang X, et al. Strategies to prevent, curb and eliminate biofilm formation based on the characteristics of various periods in one biofilm life cycle. *Front Cell Infect Microbiol*. 2022;12:1–18. doi:10.3389/fcimb.2022.1003033
2. McCarty S, Woods E, Percival SL. Biofilms: from concept to reality. In: *Biofilms in Infection Prevention and Control*. Elsevier; 2014:143–163. doi:10.1016/B978-0-12-397043-5.00009-8
3. Zafer MM, Mohamed GA, Ibrahim SRM, Ghosh S, Bornman C, Elfaky MA. Biofilm-mediated infections by multidrug-resistant microbes: a comprehensive exploration and forward perspectives. *Arch Microbiol*. 2024;206(3):101. doi:10.1007/s00203-023-03826-z
4. Yang S, Li X, Cang W, et al. Biofilm tolerance, resistance and infections increasing threat of public health. *Microb Cell*. 2023;10(11):233–247. doi:10.15698/mic2023.11.807
5. Davies D. Understanding biofilm resistance to antibacterial agents. *Nat Rev Drug Discov*. 2003;2(2):114–122. doi:10.1038/nrd1008
6. Prinzi A, Rohde R The role of bacterial biofilms in antimicrobial resistance. American Society for Microbiology. March 6, 2023. Available from: https://asm.org/articles/2023/march/the-role-of-bacterial-biofilms-in-antimicrobial-re. Accessed September 12 2024.
7. Billings N, Ramirez Millan M, Caldara M, et al. The extracellular matrix component psl provides fast-acting antibiotic defense in pseudomonas aeruginosa biofilms. *PLoS Pathog*. 2013;9(8):e1003526. doi:10.1371/journal.ppat.1003526
8. Hall CW, Mah TF. Molecular mechanisms of biofilm-based antibiotic resistance and tolerance in pathogenic bacteria. *FEMS Microbiol Rev*. 2017;41(3):276–301. doi:10.1093/femsre/fux010
9. Sun F, Qu F, Ling Y, et al. Biofilm-associated infections: antibiotic resistance and novel therapeutic strategies. *Future Microbiol*. 2013;8(7):877–886. doi:10.2217/fmb.13.58
10. Saleh A, Akkuş-Dağdeviren ZB, Haddadzadegan S, Wibel R, Bernkop-Schnürch A. Peptide antibiotic–polyphosphate nanoparticles: a promising strategy to overcome the enzymatic and mucus barrier of the intestine. *Biomacromolecules*. 2023;24(6):2587–2595. doi:10.1021/acs.biomac.3c00083
11. Hock N, To D, Armengol ES, et al. Design of biodegradable nanoparticles for enzyme-controlled long-acting drug release. *J Drug Deliv Sci Technol*. 2023;89:105085. doi:10.1016/j.jddst.2023.105085
12. Saleh A, Akkuş-Dağdeviren ZB, Friedl JD, Knoll P, Bernkop-Schnürch A. Chitosan – polyphosphate nanoparticles for a targeted drug release at the absorption membrane. *Heliyon*. 2022;8(9):e10577. doi:10.1016/j.heliyon.2022.e10577
13. Akkuş-Dağdeviren ZB, Saleh A, Schöpf C, et al. Phosphatase-degradable nanoparticles: a game-changing approach for the delivery of antifungal proteins. *J Colloid Interface Sci*. 2023;646:290–300. doi:10.1016/j.jcis.2023.05.051
14. Le NMN, Steinbring C, Le-Vinh B, Jalil A, Matuszczak B, Bernkop-Schnürch A. Polyphosphate coatings: a promising strategy to overcome the polycation dilemma. *J Colloid Interface Sci*. 2021;587:279–289. doi:10.1016/j.jcis.2020.12.019
15. Le-Vinh B, Akkuş-Dağdeviren ZB, Le NN, Nazir I, Bernkop-Schnürch A. Alkaline phosphatase: a reliable endogenous partner for drug delivery and diagnostics. *Adv Ther*. 2022;5(2):2100219. doi:10.1002/adtp.202100219
16. El-Sayed Ahmed MAEG, Zhong LL, Shen C, Yang Y, Doi Y, Tian GB. Colistin and its role in the Era of antibiotic resistance: an extended review (2000–2019). *Emerg Microbes Infect*. 2020;9(1):868–885. doi:10.1080/22221751.2020.1754133

17. Si W, Wang L, Usongo V, Zhao X, Yarden O, Li S. Colistin Induces S. aureus Susceptibility to Bacitracin. *Front Microbiol*. 2018;9:9. doi:10.3389/fmicb.2018.02805
18. Klinger-Strobel M, Stein C, Forstner C, Makarewicz O, Pletz MW. Effects of colistin on biofilm matrices of Escherichia coli and Staphylococcus aureus. *Int J Antimicrob Agents*. 2017;49(4):472–479. doi:10.1016/j.ijantimicag.2017.01.005
19. Rodriguez-Nava G, Mohamed A, Yanez-Bello MA, Trelles-Garcia DP. Advances in medicine and positive natural selection: prosthetic valve endocarditis due to biofilm producer micrococcus luteus. *IDCases*. 2020;20:e00743. doi:10.1016/j.idcr.2020.e00743
20. Shanks D, Goldwater P, Pena A, Saxon B. Fatal micrococcus sp. infection in a child with leukaemia - A cautionary case. *Med Pediatr Oncol*. 2001;37(6):553–554. doi:10.1002/mpo.1253
21. Celiksoy V, Moses RL, Sloan AJ, Moseley R, Heard CM. Synergistic In vitro antimicrobial activity of pomegranate rind extract and zinc (II) against micrococcus luteus under planktonic and biofilm conditions. *Pharmaceutics*. 2021;13(6):851. doi:10.3390/pharmaceutics13060851
22. Ianniello NM, Andrade DC, Ivancic S, Eckardt PA, Lemos Ramirez JC. Native valve infective endocarditis due to micrococcus luteus in a non-hodgkin's lymphoma patient. *IDCases*. 2019;18:e00657. doi:10.1016/j.idcr.2019.e00657
23. Satta G, D'Andrea L, Grazi G, Soro O, Varaldo PE. Micrococci demonstrate a phosphatase activity which is repressed by phosphates and which can be differentiated from that of staphylococci. *Int J Syst Bacteriol*. 1993;43(4):813–818. doi:10.1099/00207713-43-4-813
24. Kiilll CP, da S Barud H, Santagneli SH, et al. Synthesis and factorial design applied to a novel chitosan/sodium polyphosphate nanoparticles via ionotropic gelation as an RGD delivery system. *Carbohydr Polym*. 2017;157:1695–1702. doi:10.1016/j.carbpol.2016.11.053
25. Akkuş-Dağdeviren ZB, Wolf JD, Kurpiers M, Shahzadi I, Steinbring C, Bernkop-Schnürch A. Charge reversal self-emulsifying drug delivery systems: a comparative study among various phosphorylated surfactants. *J Colloid Interface Sci*. 2021;589:532–544. doi:10.1016/j.jcis.2021.01.025
26. Ordooei Javan A, Shokouhi S, Sahraei Z. A review on colistin nephrotoxicity. *Eur J Clin Pharmacol*. 2015;71(7):801–810. doi:10.1007/s00228-015-1865-4
27. To D, Kakar A, Kali G, et al. Iminated aminoglycosides in self-emulsifying drug delivery systems: dual approach to break down the microbial defense. *J Colloid Interface Sci*. 2023;630:164–178. doi:10.1016/j.jcis.2022.10.077
28. Wibel R, Knoll P, Le-Vinh B, Kali G, Bernkop-Schnürch A. Synthesis and evaluation of sulfosuccinate-based surfactants as counterions for hydrophobic ion pairing. *Acta Biomater*. 2022;144:54–66. doi:10.1016/J.ACTBIO.2022.03.013
29. Fagerquist CK. Unlocking the proteomic information encoded in MALDI-TOF-MS data used for microbial identification and characterization. *Expert Rev Proteomics*. 2017;14(1):97–107. doi:10.1080/14789450.2017.1260451
30. Tanner H, Evans JT, Gossain S, Hussain A. Evaluation of three sample preparation methods for the direct identification of bacteria in positive blood cultures by MALDI-TOF. *BMC Res Notes*. 2017;10(1):48. doi:10.1186/s13104-016-2366-y
31. Coraça-Huber DC, Kreidl L, Steixner S, Hinz M, Dammerer D, Fille M. Identification and morphological characterization of biofilms formed by strains causing infection in orthopedic implants. *Pathogens*. 2020;9(8):649. doi:10.3390/pathogens9080649
32. European Committee for Antimicrobial Susceptibility Testing (EUCAST) ofthe European Society of Clinical Microbiology and Infectious Diseases (ESCMID). Determination of minimum inhibitory concentrations (MICs) of antibacterial agents by broth dilution. *Clin Microbiol Infect*. 2003;9(8):ix–xv. doi:10.1046/j.1469-0691.2003.00790.x
33. European Committee for Antimicrobial Susceptibility Testing (EUCAST) ofthe European Society of Clinical Microbiology and Infectious Diseases (ESCMID). Terminology relating to methods for the determination of susceptibility of bacteria to antimicrobial agents. *Clin Microbiol Infect*. 2000;6(9):503–508. doi:10.1046/j.1469-0691.2000.00149.x
34. Blakeman JT, Morales-García AL, Mukherjee J, et al. Extracellular DNA provides structural integrity to a micrococcus luteus biofilm. *Langmuir*. 2019;35(19):6468–6475. doi:10.1021/acs.langmuir.9b00297
35. Azeredo J, Azevedo NF, Briandet R, et al. Critical review on biofilm methods. *Crit Rev Microbiol*. 2017;43(3):313–351. doi:10.1080/1040841X.2016.1208146
36. Knabl L, Kuppelwieser B, Mayr A, et al. High percentage of microbial colonization of osteosynthesis material in clinically unremarkable patients. *Microbiologyopen*. 2019;8(3):1–6. doi:10.1002/mbo3.658
37. Le-Vinh B, Steinbring C, Wibel R, Friedl JD, Bernkop-Schnürch A. Size shifting of solid lipid nanoparticle system triggered by alkaline phosphatase for site specific mucosal drug delivery. *Eur J Pharm Biopharm*. 2021;163:109–119. doi:10.1016/j.ejpb.2021.03.012
38. Akkus ZB, Nazir I, Jalil A, Tribus M, Bernkop-Schnürch A. Zeta potential changing polyphosphate nanoparticles: a promising approach to overcome the mucus and epithelial barrier. *Mol Pharm*. 2019;16(6):2817–2825. doi:10.1021/acs.molpharmaceut.9b00355
39. Kantrowitz ER. E. coli Alkaline Phosphatase. In: *Encyclopedia of Inorganic and Bioinorganic Chemistry*. John Wiley & Sons, Ltd; 2011:1–13. doi:10.1002/9781119951438.eibc0479
40. Li J, Milne RW, Nation RL, Turnidge JD, Coulthard K. Stability of colistin and colistin methanesulfonate in aqueous media and plasma as determined by high-performance liquid chromatography. *Antimicrob Agents Chemother*. 2003;47(4):1364–1370. doi:10.1128/AAC.47.4.1364-1370.2003
41. Shigeta M, Tanaka G, Komatsuzawa H, Sugai M, Suginaka H, Usui T. Permeation of antimicrobial agents through pseudomonas aeruginosa biofilms: a simple method. *Chemotherapy*. 1997;43(5):340–345. doi:10.1159/000239587
42. Al-Zubairy SA. Microbiologic cure with a simplified dosage of intravenous colistin in adults: a retrospective cohort study. *Infect Drug Resist*. 2023;16:4237–4249. doi:10.2147/IDR.S411381
43. Linden PK, Kusne S, Coley K, Fontes P, Kramer DJ, Paterson D. Use of parenteral colistin for the treatment of serious infection due to antimicrobial-resistant pseudomonas aeruginosa. *Clinl Infect Dis*. 2003;37(11):e154–e160. doi:10.1086/379611
44. Katip W, Rayanakorn A, Oberdorfer P, Taruangsri P, Nampuan T. Short versus long course of colistin treatment for carbapenem-resistant A. baumannii in critically ill patients: a propensity score matching study. *J Infect Public Health*. 2023;16(8):1249–1255. doi:10.1016/j.jiph.2023.05.024
45. Yousefi Nojookambari N, Eslami G, Sadredinamin M, et al. Sub-minimum inhibitory concentrations (sub-MICs) of colistin on Acinetobacter baumannii biofilm formation potency, adherence, and invasion to epithelial host cells: an experimental study in an Iranian children's referral hospital. *Microbiol Spectr*. 2024;122. doi:10.1128/spectrum.02523-23
46. Andrade FF, Silva D, Rodrigues A, Pina-Vaz C. Colistin update on its mechanism of action and resistance, present and future challenges. *Microorganisms*. 2020;8(11):1716. doi:10.3390/microorganisms8111716

47. Farag MR, Alagawany M. Erythrocytes as a biological model for screening of xenobiotics toxicity. *Chem Biol Interact*. 2018;279:73–83. doi:10.1016/j.cbi.2017.11.007
48. Ayrapetyan M, Williams T, Oliver JD. Relationship between the viable but nonculturable state and antibiotic persister cells. *J Bacteriol*. 2018;200 (20):1–15. doi:10.1128/JB.00249-18
49. Lorencová E, Vltavská P, Budinský P, Koutný M. Antibacterial effect of phosphates and polyphosphates with different chain length. *J Environ Sci Health A*. 2012;47(14):2241–2245. doi:10.1080/10934529.2012.707544
50. Gannesen AV, Ziganshin RH, Zdorovenko EL, et al. Epinephrine extensively changes the biofilm matrix composition in micrococcus luteus C01 isolated from human skin. *Front Microbiol*. 2022;13:1–20. doi:10.3389/fmicb.2022.1003942
51. Konduri R, Saiabhilash CR, Shivaji S. Biofilm-forming potential of ocular fluid staphylococcus aureus and staphylococcus epidermidis on ex vivo human corneas from attachment to dispersal phase. *Microorganisms*. 2021;9(6):1124. doi:10.3390/microorganisms9061124
52. Ciofu O, Rojo-Molinero E, Macià MD, Oliver A. Antibiotic treatment of biofilm infections. *Apmis*. 2017;125(4):304–319. doi:10.1111/apm.12673
53. Liu YH, Kuo SC, Yao BY, et al. Colistin nanoparticle assembly by coacervate complexation with polyanionic peptides for treating drug-resistant gram-negative bacteria. *Acta Biomater*. 2018;82:133–142. doi:10.1016/j.actbio.2018.10.013
54. Muenraya P, Sawatdee S, Srichana T, Atipairin A. Silver nanoparticles conjugated with colistin enhanced the antimicrobial activity against gram-negative bacteria. *Molecules*. 2022;27(18):5780. doi:10.3390/molecules27185780
55. Scutera S, Argenziano M, Sparti R, et al. Enhanced antimicrobial and antibiofilm effect of new colistin-loaded human albumin nanoparticles. *Antibiotics*. 2021;10(1):57. doi:10.3390/antibiotics10010057
56. Akkuş-Dağdeviren ZB, Fürst A, David Friedl J, Tribus M, Bernkop-Schnürch A. Nanoarchitectonics of Layer-by-Layer (LbL) coated nanostructured lipid carriers (NLCs) for enzyme-triggered charge reversal. *J Colloid Interface Sci*. 2023;629:541–553. doi:10.1016/j.jcis.2022.08.190